

Fabrication and characterization of silicon-based 3D electrodes for high energy lithium-ion batteries

Y. Zheng^{*,1}, P. Smyrek^{1,2}, J.-H. Rakebrandt¹, Ch. Kübel³, H.J. Seifert¹, W. Pfleging^{1,2}

¹ *Institute for Applied Materials - Applied Materials Physics, Karlsruhe Institute of Technology, P.O. Box 3640, 76021 Karlsruhe, Germany*

² *Karlsruhe Nano Micro Facility, H.-von-Helmholtz-Platz 1, 76344 Egg.-Leopoldshafen, Germany*

³ *Institute of Nanotechnology, Karlsruhe Institute of Technology, H.-von-Helmholtz-Platz 1, 76344 Egg.-Leopoldshafen, Germany*

ABSTRACT

For next generation of high energy lithium-ion batteries, silicon as anode material is of great interest due to its higher specific capacity (3579 mAh/g). However, the volume change during de-/intercalation of lithium-ions can reach values up to 300 % causing particle pulverization, loss of electrical contact and even delimitation of the composite electrode from the current collector. In order to overcome these drawbacks for silicon anodes we are developing new 3D electrode architectures. Laser nano-structuring of the current collectors is developed for improving the electrode adhesion and laser micro-structuring of thick film composite electrodes is applied for generating of freestanding structures. Freestanding structures could be attributed to sustain high volume changes during electrochemical cycling and to improve the capacity retention at high C-rates (> 0.5 C). Thick film composite Si and Si/graphite anode materials with different silicon content were deposited on current collectors by tape-casting. Film adhesion on structured current collectors was investigated by applying the 90 °peel-off test. Electrochemical properties of cells with structured and unstructured electrodes were characterized. The impact of 3D electrode architectures regarding cycle stability, capacity retention and cell life-time will be discussed in detail.

Keywords: lithium-ion battery, ultrafast laser ablation, micro/nano-structuring, silicon anode, film adhesion

1. INTRODUCTION

For the next generation lithium-ion battery with high power and energy density, advanced cathode and anode materials are urgently required. Among different anode materials, silicon with high theoretic capacity has been regarded as one of the most promising anode materials. Silicon as anode has high theoretic capacity of 3579 mAh/g (formation of $\text{Li}_{15}\text{Si}_4$ phase) at room temperate and a moderate potential of 0.4 V (Li/Li⁺) [1]. In addition, lithiated silicon in the electrolyte is more stable and saver than common lithiated graphite [1]. Major challenge for commercializing of silicon based anode materials is short lifespan, cycle stability and capacity retention because of huge volume change of about 300% during electrochemical cycling [2, 3]. The most reported failure mechanisms leading to rapid capacity loss are cracking or pulverisation of silicon particles during electrochemical cycling [4]. Solid electrolyte interphase (SEI) is continuously formed on the electrode surface which is exposed to the liquid electrolyte. As a results, the electrolyte decomposes and the thickness of SEI increases which leads to increased impedance [5]. In order to stabilize the SEI layer, fluoroethylene carbonate (FEC) and vinylene carbonate (VC) are added to the liquid electrolyte [6, 7]. Furthermore, due to volume contraction the silicon particles will lose their electric contact with surrounding particles and the electrode film will partially show lift-off from current collector.

To overcome the drawbacks of silicon-based anode material, 3D freestanding structures are generated on electrode materials by applying ultrafast laser ablation. Free space from 3D patterns can compensate the volume change and reduce the mechanic stress inside of the electrode. To investigate the electrochemical properties, electrodes with and without 3D architecture were assembled in cells with Swagelok[®] design and subsequently galvanostatic measurements were performed. For improving of film adhesion between the electrode material and the current collector, ultrafast laser patterning was used to generate nano/micro-sized surface structures. The increased active surface area can enhance the mechanic anchoring of the electrode material towards the current collector.

*yijing.zheng@kit.edu; phone +49 (0)721 608 22936; fax +49 (0)721 608 24567, <http://www.iam.kit.edu/awp/146.php>

1.1 Characterizing of silicon nanoparticles

In order to achieve high specific capacity, crystalline silicon nanopowder (MTI Corporation, USA) with an average particle size of 100 nm was purchased for synthesis of composite anode materials. Before fabricating of electrode slurry, the chemical composition of silicon nanoparticles was analyzed by means of inductively coupled plasma optical emission spectrometry (ICP-OES). It was shown, that the silicon nano-powder contains a huge oxygen proportion of about 34 wt%. TEM-images (fig. 1) indicate that a native oxide layer was formed on the silicon particles. The formation of silicon oxide can induce a lower specific discharge capacity but the oxide layer can also act as buffering phase regarding an alleviation of mechanical stresses during electrochemical cycling [1].

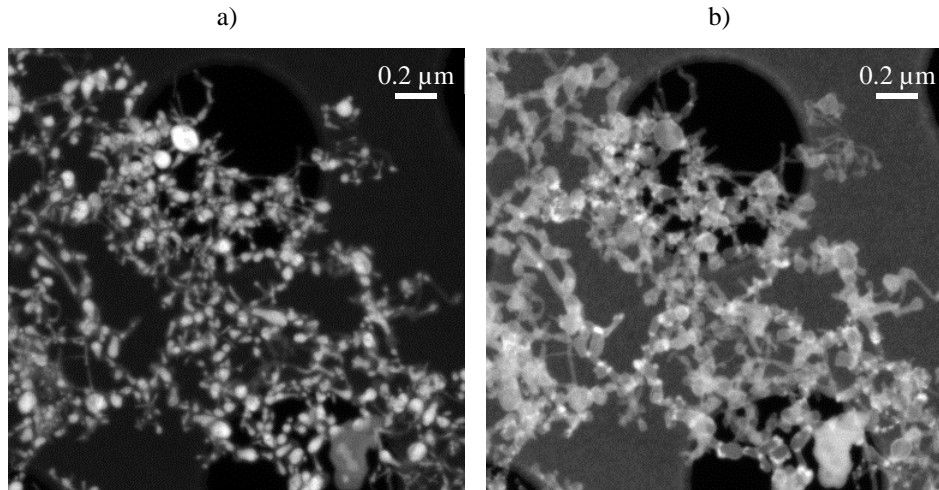


Figure 1: Energy filtered TEM of a silicon powder. The filter was set at 17 eV (a) and 24 eV (b) making use of the plasmon energy of silicon and silicon dioxide, respectively. In (a) silicon appears bright and silicon dioxide appears dark. Inversed contrast is given in (b).

1.2 Preparation of electrode material

In order to achieve high specific capacity, crystalline silicon nanoparticles (MTI Corporation, USA) with an average particle size of 100 nm were used for synthesis of composite anode materials. 3D architectures were generated in silicon-based electrodes by using ultrafast laser ablation. Two types of binder were used, carboxymethylcellulose (CMC) added with styrene-butadiene rubber (SBR) (MTI corporation, USA) and poly(acrylic acid) (PAA) (Aldrich, USA). The chemical composition of different composite materials is summarized in Table 1. The silicon anode slurry consisted of silicon nanopowder, binder, conductive agent (Timcal Super C65, MTI Corporation, USA) and distilled water as solvent. For Si/C composite materials, graphite (Targray Technology International Inc., USA) was added additionally. A high-speed mixer (Filmix, Primix, Japan) was applied to disperse and mix the electrode materials and could ensure homogenous distribution of nano-sized particles. Subsequently, the silicon-based anode composited electrode materials were coated on 12 μm thick copper foil (Targray technology, USA) by using a tape-casting film coater (Model: MSK-AFA-L800-H, MTI Corporation, USA). The coated electrodes were dried up by using a heating lid at ~ 60 °C in ambient air for 1 hours. All the films were calendared by using a compact hot rolling press (Precision 4" Hot Rolling Press/Calender, MTI Corporation, USA). After calendaring, the film thickness of Si- and Si/C anodes were adjusted to 25 – 30 μm and 50 – 60 μm, respectively.

Table 1: composition of various types of silicon-based composite materials.

Binder	Silicon (wt%)	Graphite (wt%)	Carbon black (wt%)	Binder (wt%)	Spec. capacity* (mAh/g)
CMC + SBR (1:1)	10	-	70	20	3579
	40	-	40	20	3579
	10	70	10	10	727
	20	60	10	10	1135
PAA	33	-	33	33	3579
	10	70	10	10	727

* related to mass of active materials

1.3 Ultrafast laser processing for 3D electrodes

The used ultrafast fiber laser source (Tangerine, Amplitude Systèmes, France) operates at central wavelength of 1030 nm with a maximum average laser power of 35 W and adjustable repetition rate in a range of 1 Hz up to 2 MHz. The laser pulse duration can be tuned from 350 fs to 10 ps. By means of second harmonic generation, the visible irradiation with a wavelength of 515 nm and a pulse duration of 380 fs was applied for fabrication of freestanding structures on the silicon-based composite anode materials. Regarding to film adhesion, dot patterns with varying pitch distance were generated on copper surface. Due to single laser pulse irradiation, nano-sized pores and ripple structures were formed.

1.4 Electrochemical characterization

For electrochemical testing Swagelok® cells using Li as counter and reference electrode and a silicon-based working electrode were assembled with a glass fiber separator (GF/A Whatman) in an argon-filled glove box. 1.3M solution of lithium hexafluorophosphate (LiPF₆) in ethyle carbonate (EC) and ethyl methyl carbonate (EMC) with a weight ratio of 3:7 was used. 5 wt% of fluoroethylene carbonate (FEC) is additionally added in order to achieve a stable solid-electrolyte interphase (SEI) on anode surface. Before cell assembly, the electrodes were heated at 130 °C for 24 h in vacuum oven. Galvanostatic measurements were performed using a BT2000 battery cycler (Arbin Instruments, USA) at room temperature with a cut-off voltage in the range of 0.01 to 2 and 0.01 to 1.5 V for silicon anode and silicon/graphite anode respectively. After five formation cycles, the galvanostatic testing was carried out with increasing C-rates from 0.1 C up to 3C for 10 cycles. Subsequently, the cells were cycled at a rate of 0.2 C for 100 cycles, in order to study cycle stability and capacity retention at room temperature.

1.5 90° peel-off adhesion test

90° peel-off tests were applied in order to evaluate the tensile strength between the composite coating and the current collector. For this purpose an adhesion tester device was used, which is embedded in an universal testing machine (10T, UTS, Germany). The electrode materials were stuck to the adhesive tape on the substrate. Using a mechanical clamp, the end of the electrode film was fixed to a mechanical testing machine load cell. Tensile force is oriented perpendicular to the peeled electrode films. During the measurement, the substrate was moving with a testing speed of 600 mm/min. The force needed to separate the electrode material from the current collector was measured. The tensile strength γ is calculated from the measured tensile force F related to the width d of sample, which is equal to equation (1):

$$\gamma = F/d \quad (1)$$

Silicon/graphite (20 wt%:60 wt%) anode material was deposited on the glossy and laser structured copper foil in order to investigate the influence of current collector surface topography on film adhesion.

2. RESULTS AND DISCUSSION

2.1 Formation of laser-assisted surface structures

After coating process, the freestanding structures were generated with a pitch distance of $100\ \mu\text{m}$ (Fig. 2). In order to achieve maximum aspect ratio and reduce the loss of active material, a lower laser fluence of $0.44\ \text{J}/\text{cm}^2$ was used and the laser processing was repeated until the materials were ablated down to copper current collector. None of melt formation could be observed after laser processing.

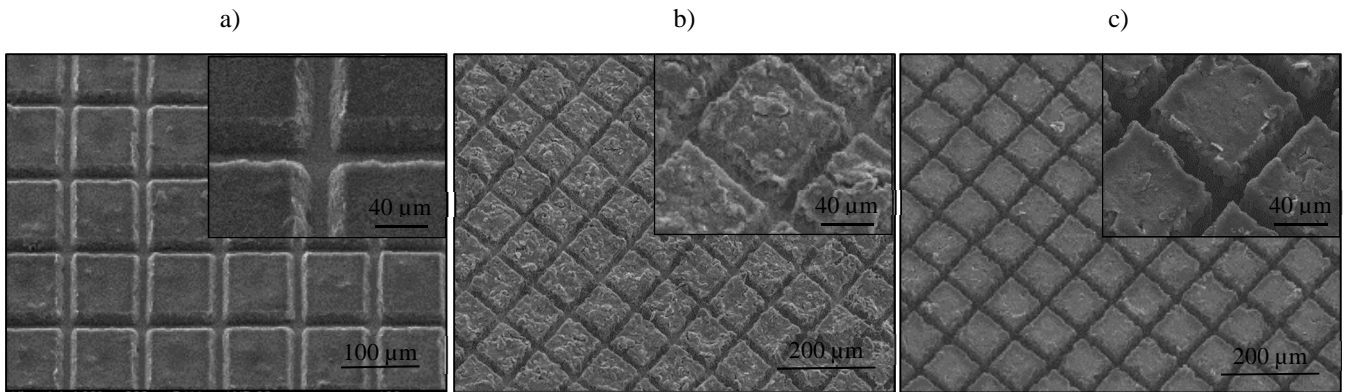


Figure 2: SEM-images of silicon-based composite anode materials: a) silicon anode (binder: CMC and SBR), b) silicon/graphite anode (binder: CMC and SBR), c) silicon/graphite anode (binder: PAA). Laser fluence: $0.44\ \text{J}/\text{cm}^2$

2.2 Electrochemical characterization

In order to investigate electrochemical performance of structured and unstructured anode materials, galvanostatic measurements with different C-rates were performed. During formation step, a C-rate of $C/20$ was applied for 5 full-cycles. Subsequently, the discharge time from the last cycle and the formation current were used to calculate the practical C-rate, which is needed to fully charge and discharge the cells in 1 hour in practice. Afterwards, all cells were cycled with increasing C-rate ($C/10$, $C/5$, $C/2$, C , $2C$, $3C$) and finally the charge/discharge current was reduced to $C/5$ in order to investigate the electrochemical degradation and capacity retention.

- **Silicon anode**

Specific discharge capacity of silicon anode with different silicon content as function of cycle number is shown in figure 3. For structured and unstructured cells with 40 wt.% silicon, similar specific capacity of about $2850\ \text{mAh}/\text{g}$ during first lithiation was achieved. During this first cycle, the solid electrolyte interface (SEI) film was formed on the silicon electrode surface. The specific discharge capacity of the cell with unstructured electrode fades quickly within the first few cycles (during formation step). With increasing C-rate, discharge capacity decreases successively. A dramatic capacity drop was observed if the C-rate was increased to $1C$ and $2C$. Finally, the C-rate was decreased to $C/5$ and it was observed, that the specific discharge capacity could not gain the value from the beginning of electrochemical testing. This is due to degradation processes during cycling at high C-rate. In comparison to the cell with unstructured electrode, the cell with structured electrode containing freestanding structures shows an improved electrochemical performance and higher capacity, although the specific discharge capacity drops with increasing C-rate. However, a discharge capacity larger than $1000\ \text{mAh}/\text{g}$ could be reached at $3C$ and a significantly decreased degradation at the end of the galvanostatic testing at reduced C-rate ($C/5$) was detected.

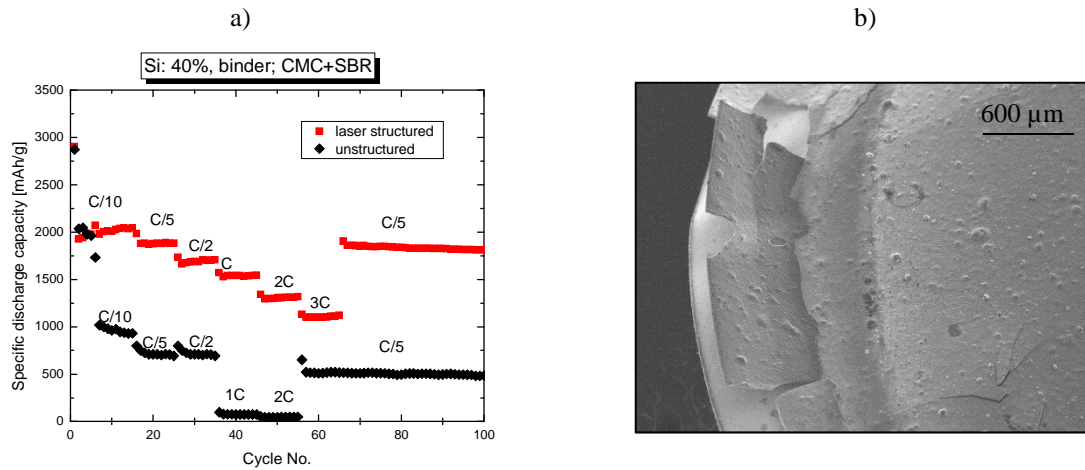


Figure 3: Specific discharge capacity as function of cycle number of structured and unstructured cells (a) and SEM image of silicon anode (b) (Si: 40%, binder CMC+SBR) after 100 cycles.

After battery test, the Swagelok® cell with unstructured electrode was disassembled and washed in DMC solution for 1 h. Post-mortem-analysis was applied, in order to investigate mechanical degradation of the electrode. SEM image (figure 3b) show that electrode material was delaminated from the current collectors and crack formation occurred on the electrode surface. These processes are responsible for the capacity drop observed during cell testing (figure 3a).

- **Silicon/ graphite anode**

In the silicon/graphite anode, silicon is embedded in the matrix of graphite in order to find an appropriate compromise regarding volume change, capacity and cycle lifetime [8]. Figure 4 shows the specific discharge capacity for cells with un-/structured electrodes, which were fabricated with two different types of binder. Similar to cells with unstructured silicon anode, the major issue of cells with unstructured silicon/graphite anode is the dramatic capacity fading at high C-rates (> 1C). An improved capacity retention and increased specific capacity, especially for higher C-rates, can be obtained for cells with structured electrodes. These cells also show an excellent long/term cycling stability in comparison to cells with unstructured electrodes. Anyway, the graphite anode doped with Si (10 wt%) can deliver significant higher specific capacities in comparison to conventional graphite anodes.

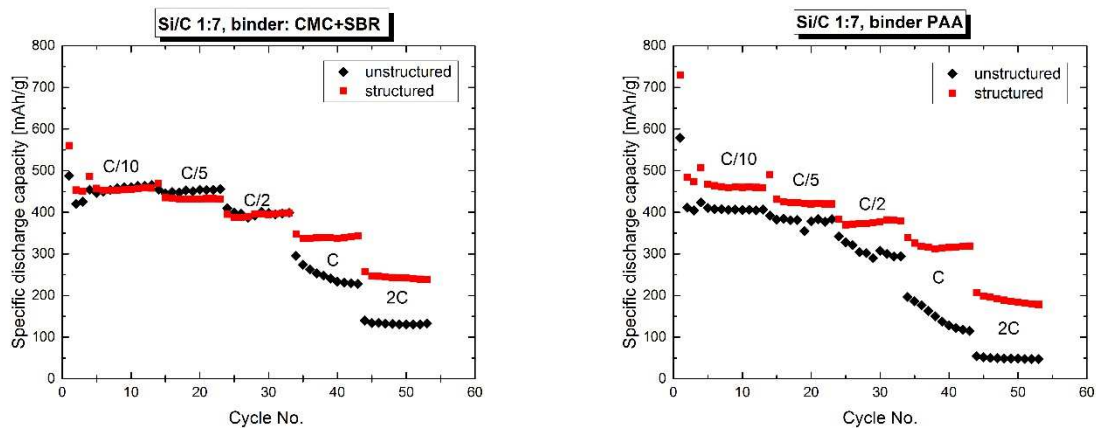


Figure 4: Specific discharge capacity as function of cycle number for structured and unstructured cells applying CMC+SBR and PAA as binder.

Due to laser generated free space, volume changes during insertion and extraction of lithium-ions were compensated and thus mechanical stress inside of electrode was reduced. These factors contribute to an improved capacity retention and

battery performance. Furthermore, laser modified 3D structures can reduce the lithium-ion diffusion path length from bulk materials across the active surface to the electrolyte and vice versa and therefore the increased lithium-ion transport kinetic leads to an improved capacity retention at high C-rates [9].

In this work, theoretic specific capacity of 3579 mAh/g was not achieved which might be due to the significant amount of oxygen content [1] and also micro-sized agglomeration of silicon particles might induce a drop in capacity [10]. Thick oxide shell on the silicon surface can prevent silicon from expanding, but it limits also the lithiation process.

2.3 Measurement of adhesion strength

Due to repeated volume expansion/contraction during prolonged cycles, the electrode film was delaminated from the current collector (Fig. 3b). An improvement of film adhesion is required in order to avoid capacity fading. For this propose, dot patterns (Fig. 5b) with various pitch distance (25 μm and 50 μm) were generated. Figure 5a depicts the tensile strength of the composite layer on the laser structured copper surfaces as function of pitch distance compared to the untreated surface (“reference”). In comparison to the reference, the film adhesion could not be increased by applying dots patterns which is due to an insufficient intrinsic film stability or a weak mechanical strength among binder and particles. This is called “cohesion failure” inside the coating [8]. However, after tensile strength measurement, a significant increased amount of graphite particles, which remain on the laser modified current collector foil was observed in comparison to the reference (Fig. 5a). In order to further investigate the influence of film adhesion on surface structures, the amount of residual particles on the current collectors were evaluated and calculated by contrast analysis of the SEM images. The contrast analysis of SEM images is based on the different brightness of components and materials on the substrate. Graphite particles and exposed copper surface were represented in red and green color, respectively (Fig. 6 b,d). The surface percentage of residual graphite particles and that of Cu were calculated. Hereby, the structured current collector with a dot period of 50 μm reveals the largest amount of residual graphite particles. Dot patterns with nano-sized pore structures act as anchor for improving mechanical adhesion towards to current collector. Additionally, the surface percentage of residual graphite particles could serve as an index on evaluating the adhesive force between Cu foil and anode film.

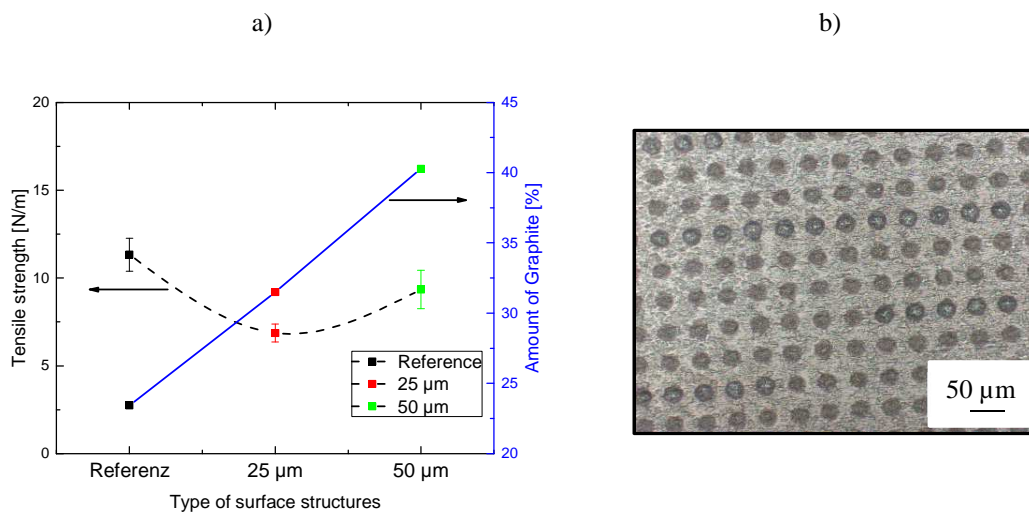


Figure 5: (a) tensile strength of Si/graphite anode films and amount of graphite particles (surface percentage) after 90° peel-off test as function of surface pattern (dot patterns with different pitch distance and reference) and (b) light microscopy image of laser induced dot structure (pitch distance: 50 μm , electrode: Si/C, binder: CMC+SBR).

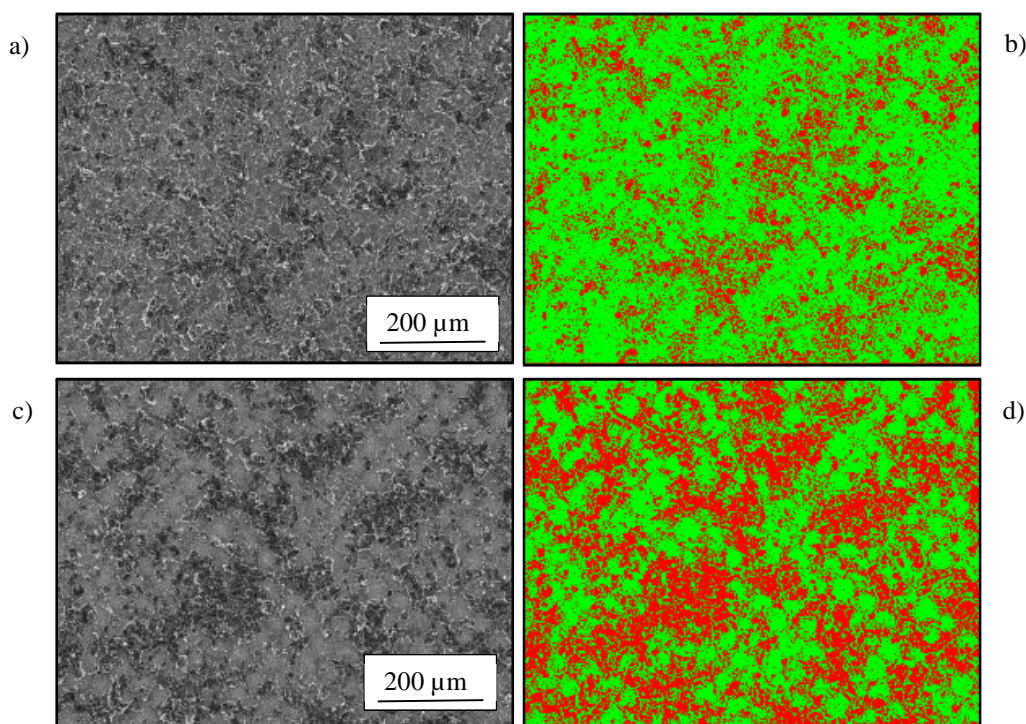


Figure 6: SEM images (a,c) and corresponding contrast images (b,d) of reference (a,b) and laser structured (c,d) copper foils after 90° peel-off tests (pitch distance 50 μm).

3. CONCLUSIONS

In this study, various types of silicon-based composite materials were fabricated. Freestanding structures on the electrodes without melt formation were realized by ultrafast laser ablation. Galvanostatic measurements of cells with un-/structured electrodes were performed with increasing C-rate and electrochemical performance and degradation of the electrodes were evaluated. All cells with structured electrodes show improved specific discharge capacity and capacity retention, especially at high C-rate capacity retention. Post-mortem analysis reveals that unstructured electrode materials delaminated from current collector foil due to huge volume change during electrochemical cycling, which led to significant capacity fading. Dot patterns with nano-sized pore structures were generated on the copper foil in order to overcome lack of film adhesion between active materials and current collectors. Brightness contrast analysis of copper current collector foil after 90° peel-off testing indicates an enhanced amount of remaining particles. This means that laser generated nano structures act as anchor for active materials and enable an enhanced electrical contact between the particles and the current collector.

ACKNOWLEDGMENTS

We are grateful to our colleagues Zhenhua An, Chantal Rietdorf, and Stefan Pflöging for their technical assistance during laser material processing, SEM, and tensile strength measurements. This project has received funding from the European Union's Horizon 2020 research and innovation programme under the Marie Skłodowska-Curie grant agreement no. 644971. In addition, the support for laser materials processing by the Karlsruhe Nano Micro Facility (<http://www.knmf.kit.edu/>) a Helmholtz research infrastructure at KIT, is gratefully acknowledged.

REFERENCES

- [1] Ashuri, M., He, Q., and Shaw, L. L., "Silicon as a potential anode material for Li-ion batteries: where size, geometry and structure matter," *Nanoscale*, 8(1), 74-103 (2016).
- [2] Obrovac, M. N., and Krause, L. J., "Reversible cycling of crystalline silicon powder," *Journal of the Electrochemical Society*, 154(2), A103-A108 (2007).
- [3] Ma, D. L., Cao, Z. Y., and Hu, A. M., "Si-Based Anode Materials for Li-Ion Batteries: A Mini Review," *Nano-Micro Letters*, 6(4), 347-358 (2014).
- [4] Zhang, W. J., "A review of the electrochemical performance of alloy anodes for lithium-ion batteries," *Journal of Power Sources*, 196(1), 13-24 (2011).
- [5] Yoon, T., Nguyen, C. C., Seo, D. M., and Lucht, B. L., "Capacity Fading Mechanisms of Silicon Nanoparticle Negative Electrodes for Lithium Ion Batteries," *Journal of the Electrochemical Society*, 162(12), A2325-A2330 (2015).
- [6] Young, B. T., Heskett, D. R., Nguyen, C. C., Nie, M. Y., Woicik, J. C., and Lucht, B. L., "Hard X-ray Photoelectron Spectroscopy (HAXPES) Investigation of the Silicon Solid Electrolyte Interphase (SEI) in Lithium-Ion Batteries," *Acs Applied Materials & Interfaces*, 7(36), 20004-20011 (2015).
- [7] Nguyen, C. C., and Lucht, B. L., "Comparative Study of Fluoroethylene Carbonate and Vinylene Carbonate for Silicon Anodes in Lithium Ion Batteries," *Journal of the Electrochemical Society*, 161(12), A1933-A1938 (2014).
- [8] Haselrieder, W., Westphal, B., Bockholt, H., Diener, A., Hoft, S., and Kwade, A., "Measuring the coating adhesion strength of electrodes for lithium-ion batteries," *International Journal of Adhesion and Adhesives*, 60, 1-8 (2015).
- [9] Mangang, M., Seifert, H. J., and Pfleging, W., "Influence of laser pulse duration on the electrochemical performance of laser structured LiFePO₄ composite electrodes," *Journal of Power Sources*, 304, 24-32 (2016).
- [10] McDowell, M. T., Ryu, I., Lee, S. W., Wang, C. M., Nix, W. D., and Cui, Y., "Studying the Kinetics of Crystalline Silicon Nanoparticle Lithiation with In Situ Transmission Electron Microscopy," *Advanced Materials*, 24(45), 6034-6041 (2012).